Full paper / Mémoire

Monotopic binding modes for ditopic ligands: synthesis and characterization of $W_6S_8L_6$ (L = bis(diphenylphosphino)ethane, 4,4′-bipyridine) cluster compounds

Catherine M. Oertel, Lori L. Rayburn [1], Song Jin [2], Francis J. DiSalvo *

Department of Chemistry and Chemical Biology, Cornell University, Ithaca, NY 14853, USA

Abstract

We have synthesized two compounds, W_6S_8[bis(diphenylphosphino)ethane]$_6$ (**1**) and W_6S_8(4,4′-bipyridine)$_6$ (**2**), in which ditopic ligands associate with the W_6S_8 cluster in monotopic fashion. Compound **1** was synthesized through ligand exchange on W_6S_8(tbp)$_6$ (tbp = 4-*tert*-butylpyridine) in benzene and crystallized in the $R\bar{3}$ space group with $a = b = 29.7159(13)$ Å and $c = 14.2188(9)$ Å. Compound **2** was synthesized by ligand exchange on W_6S_8(tbp)$_6$ in aniline and crystallized as **2**•5aniline in the $P\bar{1}$ space group with $a = 9.3565(6)$ Å, $b = 15.7743(10)$ Å, $c = 15.8149(11)$ Å, $\alpha = 99.5975(18)°$, $\beta = 98.4930(17)°$, and $\gamma = 96.1659(18)°$. ***To cite this article: C.M. Oertel et al., C. R. Chimie 8 (2005)***.
© 2005 Académie des sciences. Published by Elsevier SAS. All rights reserved.

Résumé

Nous avons synthétisé deux composés, W_6S_8[bis(diphenylphosphino)ethane]$_6$ (**1**) et W_6S_8(4,4′-bipyridine)$_6$ (**2**) dans lesquels les ligands bidentes sont coordinés au cluster W_6S_8 de façon monodente. Le composé **1** est synthétisé par échange des ligands du cluster W_6S_8(tbp)$_6$ (tbp = 4-*tert*-butylpyridine) dans le benzène et cristallise dans le groupe d'espace $R\bar{3}$ avec $a = b = 29,7159(13)$ Å et $c = 14,2188(9)$ Å. Le composé **2** est synthétisé par échange des ligands du cluster W_6S_8(tbp)$_6$ dans l'aniline et cristallise sous la forme **2**•5aniline dans le groupe d'espace $P\bar{1}$ avec $a = 9,3565(6)$ Å, $b = 15,7743(10)$ Å, $c = 15,8149(11)$ Å, $\alpha = 99,5975(18)°$, $\beta = 98,4930(17)°$ et $\gamma = 96,1659(18)°$. ***Pour citer cet article : C.M. Oertel et al., C. R. Chimie 8 (2005)***.
© 2005 Académie des sciences. Published by Elsevier SAS. All rights reserved.

* Corresponding author.

E-mail addresses: cmo25@cornell.edu (C.M. Oertel), lori.rayburn@kodak.com (L.L. Rayburn), jin@chem.wisc.edu (S. Jin), fjd3@cornell.edu (F.J. DiSalvo).

[1] Present address: Eastman Kodak Company, Rochester, NY 14650, USA.

[2] Present address: Department of Chemistry, University of Wisconsin-Madison, 1101 University Avenue, Madison, WI 53706, USA.

1. Introduction

Group VI octahedral metal clusters of the form $M_6Q_8L_6$ (M = Mo, W; Q = S, Se, Te; L = Lewis-basic organic ligand) have been the subject of much interest over the last few decades. Since these soluble, molecular clusters became accessible due to the work of Saito et al. [1,2] and McCarley et al. [3,4], research has been directed toward understanding their synthesis [5,6], electrochemistry [7,8], and ligand exchange chemistry [9,10]. One reason for the great interest in these cluster species has been their structural relationship to the fascinating molybdenum-based Chevrel phases, which are well-known for their superconductivity [11,12], fast-ion conductivity [13,14], and catalytic properties [15,16]. In addition, theoretical work [17,18] has shown that organic-inorganic network materials built from $M_6Q_8L_6$ building blocks might also be expected to have interesting electronic and/or magnetic properties.

We have been interested in using ditopic nitrogen- and phosphorus-based ligands to build networks of covalently linked W_6S_8 clusters. This cluster core is inert except at high temperatures or under very basic conditions [19], while its axial ligands become labile under much more mild conditions, making ligand exchange a pathway to a range of W_6S_8-based compounds. Conceptually, construction of a network compound could be achieved by replacing the six monotopic ligands (L) on a molecular cluster with three equivalents of a ditopic ligand. Each bridging ligand would be shared between two clusters, leading to a three-dimensional network. In practice, this ditopic coordination has often produced insoluble, amorphous materials that are difficult to characterize [20,21]. We have also observed competing monotopic binding modes for ditopic ligands, which can result in molecular, zero-dimensional compounds. A $Re_6Se_8^{2+}$ cluster compound with monotopically bound 4,4′-bipyridine ligands has been prepared previously [22], but compounds with this mode of coordination have not been reported for the group VI clusters. The synthesis and characterization of two such compounds, $W_6S_8L_6$

(L = bis(diphenylphosphino)ethane, 4,4′-bipyridine) is reported here, along with a discussion of the interplay between ditopic and monotopic binding modes for these two ligands.

2. Experimental

2.1. General

All manipulations were carried out inside an argon-filled dry box, unless otherwise indicated. Benzene, tetrahydrofuran (THF), and diethyl ether (Et_2O) were distilled from sodium benzophenone before use. Acetonitrile (MeCN) was dried over 4 Å molecular sieves and distilled. Aniline was dried over potassium hydroxide pellets and distilled under dynamic vacuum. Deuterated solvents were purchased from Cambridge Isotopes Laboratory and used as received. $W_6S_8(tbp)_6$ (tbp = 4-*tert*-butylpyridine) was prepared according to the literature procedure [5]. Bis(diphenylphosphino)ethane (dppe) was purchased from Strem, and 4,4′-bipyridine (4,4′-bipy) was purchased from Aldrich. Both ligands were used as received. The "reaction bomb" referred to below is a custom-made, thick-walled glass vessel equipped with a Teflon valve.

^{1}H NMR spectra were collected on Varian Inova 400 and Bruker AF-300 spectrometers. Spectra were internally referenced against the residual protonated solvent peaks (δ 7.16 for benzene and δ 2.50 for DMSO). Powder X-ray diffraction was carried out on a Scintag XDS2000 diffractometer.

2.2. Synthesis of $W_6S_8[bis(diphenylphosphino)ethane]_6$ (*1*)

A reaction bomb was charged with $W_6S_8(tbp)_6$ (50 mg, 0.023 mmol), dppe (236 mg, 0.59 mmol, 25 equivalents), and benzene (8 g) to make a dark red solution. Outside the glove box, the bomb was heated in a 95 °C oil bath for 12 h, and the reaction mixture became a clear, orange–brown solution. The solution

was divided among three vials and layered with approximately equal volumes of Et$_2$O. Over a period of approximately 1 week, very small brown crystals formed at the sides and bottom of each vial. This solid was collected by filtration in air, washed with THF and Et$_2$O, and dried in vacuo. The isolated product weighed 31 mg, a 30% yield. The crystalline powder was insoluble in all organic solvents tried, including benzene, DMF, DMSO, MeCN, aniline, and THF.

2.3. Synthesis of W$_6$S$_8$(4,4′-bipyridine)$_6$ (2)

A reaction bomb was charged with W$_6$S$_8$(tbp)$_6$ (0.200 g, 0.0922 mmol), 4,4′-bipy (2.77 g, 17.7 mmol, 190 equivalents), and aniline (15 g). The vessel was removed from the glove box and heated to 100 °C for 2 days, producing a dark red reaction mixture. The mixture was filtered through a syringe filter and then layered with MeCN (25 ml) to precipitate the product. The resulting reddish-black solid was collected by filtration and washed with Et$_2$O. The isolated product weighed 0.153 g, a 60% yield. ^{1}H NMR in DMSO-d$_6$: δ 9.35 (d, 2, α-H), δ 8.77 (d, 2, β-H), δ 7.99 (d, 2, χ-H), δ 7.82 (d, 2, δ-H), all from bound 4,4′-bipy; δ 6.98 (m), δ 6.53 (m), δ 6.46 (m) and δ 4.99 (broad) from aniline; and δ 8.72 (d), δ 7.82 (d, overlapped with δ-H) from residual free 4,4′-bipy.

2.4. X-ray structure determination

Crystals of **1** suitable for single-crystal diffraction experiments were grown by layering the reaction solution described above with acetonitrile. Block-shaped, orange–brown crystals formed at the sides of the vial over a period of about 1 week. It was possible to grow block-like, dark red single crystals of **2** by layering acetonitrile on a diluted aniline reaction solution. Crystals were mounted on thin plastic loops using polybutene oil and immediately cooled in a nitrogen stream. Single-crystal diffraction data were collected on a Bruker SMART [23] system with a CCD detector using MoKα radiation. The cell parameters were initially determined using more than 50 well-centered reflections. The data were integrated using SAINT [23] software, and empirical absorption corrections were determined and applied using the SADABS [24] program. Space groups were determined through systematic absences and intensity statistics and the eventual abil-

ity to solve the structures. The structures were solved by direct methods using the SHELX [25] suite. Initial solutions, including positions of heavy atoms, were found using SHELXS, and positions of ligand atoms were determined using SHELXL to perform successive least-squares refinements on F_o^2. Crystals obtained for **1** were small and somewhat weakly diffracting, and there was a particular lack of high-angle diffraction data. The final refinement employed a SHEL command line to limit the resolution to 1.0 Å, or $2\theta = 41.6°$. Anisotropic refinement was successfully applied to the tungsten, sulfur, and phosphorus atoms in **1** and to all non-hydrogen atoms in **2**. Hydrogen atoms were added to the ligands using a riding model. Details of the crystal and refinement data for both molecules are shown in Table 1.

3. Results and discussion

3.1. Synthesis

The synthetic schemes used to prepare **1** and **2** are shown in Fig. 1. In both cases, a large excess of the ditopic ligand was used in order to assure the formation of molecular clusters and not cross-linked solids. The orange–brown reaction solution of **1** was clear, without any solid that would indicate formation of a linked product. The powder that was isolated by layering this reaction solution with Et$_2$O was surprisingly insoluble, given the initial clarity of the reaction solution. Many equivalents of excess dppe were present in the reaction solution, which could lead to increased solubility for the mixture as compared with the pure product. However, adding excess ligand to the isolated product did not increase its solubility in benzene, nor did heating the suspension. This solid has, however, been found by X-ray characterization (vide infra) to be the molecular W$_6$S$_8$(dppe)$_6$ product and not a linked product that might be expected to have low solubility. For the synthesis of **2**, the reaction mixture did contain some insoluble particles that were separated by filtration prior to crystallization of the product. Using a very large excess of 4,4′-bipy in the reaction was found to minimize formation of these impurities. W$_6$S$_8$(4,4′-bipy)$_6$ was alternatively synthesized from W$_6$S$_8$(tbp)$_6$ in a slurry of 4,4′-bipy (75 equivalents per cluster) and toluene. The mixture was heated in a sealed tube to

Table 1
Crystal and refinement data for $W_6S_8(dppe)_6$ (**1**) and $W_6S_8(4,4'\text{-bipy})_6$ (**2**)

	1	**2·5aniline**
Empirical formula	$W_6S_8C_{156}H_{144}P_{12}$	$W_6S_8C_{90}H_{83}N_{17}$
Formula weight	3749.93	2762.31
Crystal system	Trigonal	Triclinic
Space group	$R\bar{3}$	$P\bar{1}$
a (Å)	29.7159(13)	9.3565(6)
b (Å)	29.7159(13)	15.7743(10)
c (Å)	14.2188(9)	15.8149(11)
α (°)	90	99.5975(18)
β (°)	90	98.4930(17)
γ (°)	120	96.1659(18)
Volume (Å^3)	10873.5(10)	2255.3(3)
Z, calculated density (g cm^{-3})	3, 1.718	1, 2.034
μ (cm^{-1})	50.40	78.60
$F(000)$	5496	1314
Crystal size (mm^3)	$0.1 \times 0.05 \times 0.05$	$0.25 \times 0.1 \times 0.05$
Reflections collected/unique	19,828/2529	22,372/9075
Data/restraints/parameters	2529/0/144	9075/0/550
Goodness-of-fit on F_o^2	1.159	1.033
R_1^a ($I > 2\sigma$)/all data	0.0474/0.0838	0.0367/0.0521
wR_2^b ($I > 2\sigma$)/all data	0.0920/0.1038	0.0712/0.0755
Largest difference in peak and hole	0.763 and –1.012 e Å^{-3}	1.988 and –1.665 e Å^{-3}

^{a} $R_1 = \Sigma||F_o| - |F_c||/\Sigma|F_o|$.
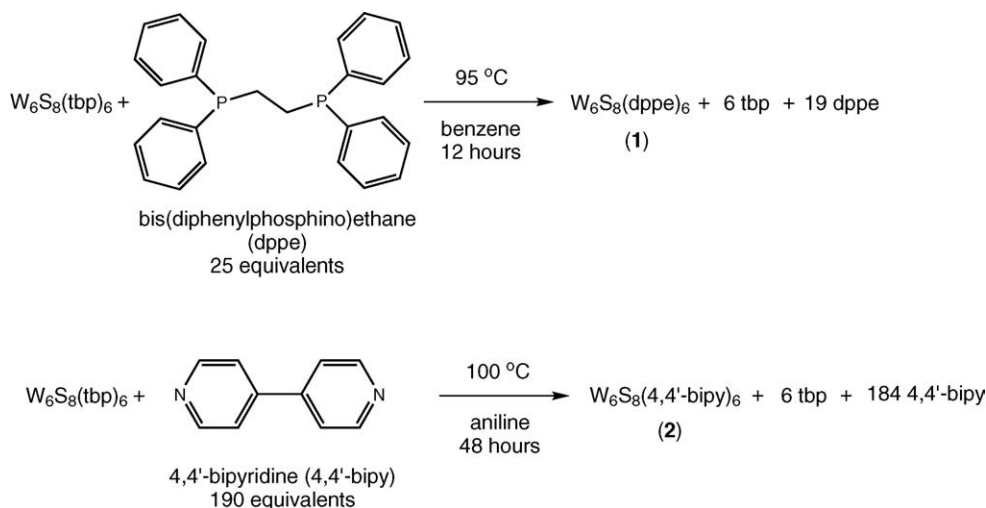^{b} $wR_2 = [\Sigma w(F_o^2 - F_c^2)^2/\Sigma w(F_o^2)^2]^{1/2}$.

Fig. 1. Synthetic schemes for $W_6S_8(dppe)_6$ (**1**) and $W_6S_8(4,4'\text{-bipy})_6$ (**2**).

125 °C and then slowly cooled to produce black needles that were determined crystallographically to be **2**·2(4,4′-bipy).

For each reaction shown in Fig. 1, a range of stoichiometries was explored in order to characterize the interplay between monotopic and ditopic ligand binding modes. At high ditopic ligand:$W_6S_8(tbp)_6$ ratios, 4,4′-bipy and dppe behave in the same way, leading exclusively to molecular, non-linked cluster species. At these stoichiometries, the competition between monotopic and ditopic binding modes is won by monotopic binding. The reaction to produce **1** was run with 25, 50, and

100 equivalents of dppe, resulting in clear reaction solutions with no evidence of precipitation. X-ray characterization of powders and/or single crystals of the reaction products showed that the monotopically coordinated product had formed. For ligand exchange involving 4,4′-bipy, formation of non-linked clusters was found to occur with the use of 20 or more equivalents of the ligand per cluster. The much larger excess (190 ligands per cluster) used in the reaction to produce **2** was found to be helpful in obtaining reproducible yields and avoiding formation of insoluble impurities.

When only a small excess of dppe or 4,4′-bipy was used in ligand exchange reactions with $W_6S_8(tbp)_6$, the two ligands were found to behave in markedly different ways. When 3–6 equivalents of 4,4′-bipy are heated with $W_6S_8(tbp)_6$ at 100 °C in benzene, the color changes from dark red to black *within minutes* of the start of heating as an amorphous compound falls out of solution. This compound cannot be recrystallized from any simple solvent system but has been determined to contain W_6S_8 clusters linked by ditopically bound 4,4′-bipy ligands [20]. By contrast, a 3:1 stoichiometric mixture of dppe and $W_6S_8(tbp)_6$ was found to maintain its dark red color for at least 1 h after the start of heating. Even after 14–18 h of heating, the solution color had changed from red–brown to orange–brown, but everything remained in solution, without a hint of precipitation. The same was observed for a 1:1 stoichiometry. For dppe, the monotopic binding mode appears to win out over ditopic binding even in the presence of a low concentration of the ditopic ligand. In addition to differing from the behavior of 4,4′-bipy, this differs from the behavior of bis(diethylphosphino)ethane (depe), which also quickly produces an insoluble, amorphous solid when reacted with $W_6S_8(tbp)_6$ in a 3:1 ratio [20]. Kinetics of substitution by the bulky dppe ligand might be expected to be slower than for the less bulky 4,4′-bipy and depe ligands. However, the almost immediate formation of amorphous products in reactions involving 4,4′-bipy and depe suggests that the linking reaction happens quickly, and some precipitate would certainly be expected after heating a reaction mixture including dppe for 18 h. The relative proximity of the two Lewis base centers on dppe is unlikely to be the origin of this behavior since one would expect similar behavior for depe, in which the two phosphine sites are also separated by an ethyl group. In fact, precipitates

readily form in the case of depe. Another possible explanation is that when a dppe ligand is monotopically bound to the W_6S_8 cluster, the remaining available phosphine site is made inaccessible to the approach of other clusters by the interaction of the bulky phenyl rings on both phosphorus atoms and on neighboring ligands. This idea is somewhat supported by the crystal structure of the $W_6S_8(dppe)_6$ molecule (vide infra).

3.2. Single-crystal structures

Both $W_6S_8(dppe)_6$ (**1**) and $W_6S_8(4,4′-bipy)_6$ (**2**) contain the W_6S_8 core, consisting of an octahedron of tungsten atoms face-capped by sulfur. ORTEP [26] representations of the asymmetric and molecular units of **1** are shown in Figs. 2 and 3, respectively. The asymmetric and molecular units of **2** may be seen in Figs. 4 and 5. Each dppe ligand in **1** is coordinated to a tungsten site through one of its phosphorus atoms. Ligands do not project straight outward from the cluster because of the 111° bends in the ethyl groups connecting the two phosphorus sites. Outer phosphorus atoms – those not coordinated to the cluster – are in close proximity to phenyl groups of other ligands on the same cluster. The crowding of these free phosphorus sites is more obvious in a space-filling model (Fig. 6). This is in contrast with the structure of **2**, in which the rigid 4,4′-bipy ligands project straight out from the cluster in each direction. Although the situation could be somewhat different in solution, this may help to explain why dppe is not as apt to bind ditopically to two clusters as is 4,4′-bipy.

Select bond length averages and ranges for **1** and **2** are shown in Table 2 in comparison with the corre-
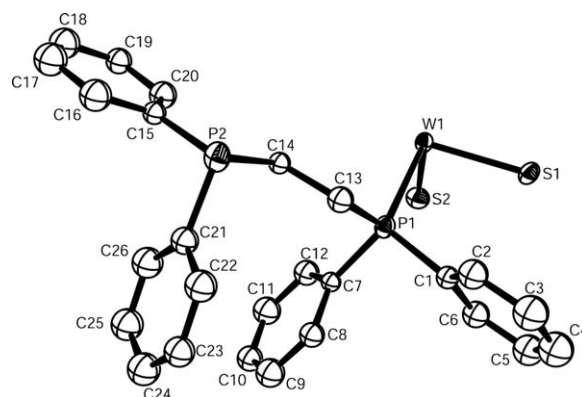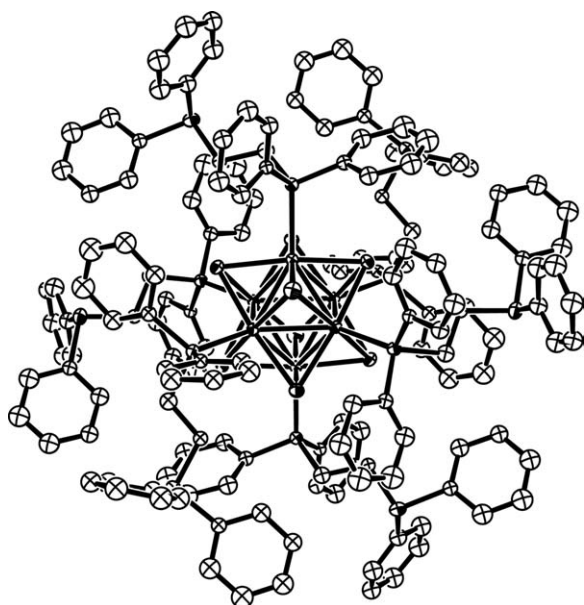

Fig. 2. Asymmetric unit of $W_6S_8(dppe)_6$ (**1**) with thermal ellipsoids drawn at 50% probability.
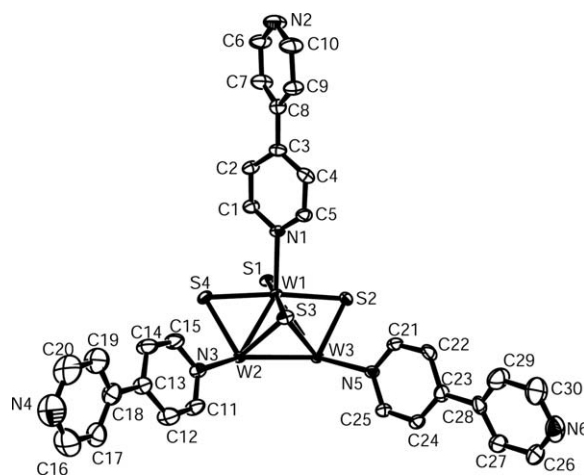
Table 2
Selected bond length ranges and averages (Å) for **1** and **2** in comparison with known W_6S_8 compounds

	1	**2**·5aniline	$W_6S_8(PEt_3)_6$[a]	$W_6S_8(PPh_3)_6$[b]	$W_6S_8(tbp)_6$[c]
W–W range	2.6802(10)–2.6817(10)	2.6581(3)–2.6685(4)	2.6759(6)–2.6813(6)	2.6749(4)–2.6899(4)	2.656(1)–2.667(1)
W–W mean[d]	2.681(1)	2.663(3)	2.679(3)	2.683(4)	2.662(6)
W–S range	2.435(5)–2.456(4)	2.4372(17)–2.4637(15)	2.451(2)–2.459(2)	2.4262(18)–2.4692(19)	2.458(2)–2.469(2)
W–S mean[d]	2.441(9)	2.450(8)	2.456(3)	2.449(12)	2.461(5)
W–L range		2.240(5)–2.263(5)		2.5561(19)–2.5915(19)	
W–L mean[d]	2.543(4)	2.251(9)	2.523(2)	2.570(12)	2.257(8)

[a] From Ref. [20].
[b] From Ref. [10].
[c] From Ref. [27].
[d] Followed by standard deviation in parentheses.

Fig. 3. Molecular unit of $W_6S_8(dppe)_6$ (**1**).

Fig. 4. Asymmetric unit of $W_6S_8(4,4'\text{-bipy})_6$ (**2**) with thermal ellipsoids drawn at 50% probability.

sponding values for three previously synthesized W_6S_8 compounds. The tungsten octahedra in all of these compounds are quite regular, and W–S distances within the cluster core do not vary much among the compounds. Larger differences may be noted in W–W and W–L distances in comparing clusters with phosphorus- and nitrogen-based ligands. The W–P bond lengths are longer than the W–N bond lengths, and the W–W distances in the phosphine compounds are longer than those in the compounds with nitrogen-based ligands. This is consistent with what has been observed within an even larger group of W_6S_8 compounds [10]. For this group of compounds, bond orders were calculated to be greater for W–P bonds than for W–N bonds, and the larger W–W distances (and smaller bond orders)

observed in phosphine compounds were attributed to the need to maintain a constant valence sum for tungsten.

Within the group of phosphine-ligated compounds, the bond lengths for **1** are similar to those reported for $W_6S_8(PPh_3)_6$ (PPh_3 = triphenylphosphine) [10] and for $W_6S_8(PEt_3)_6$ [20]. In the past, the relatively large W–L distance of 2.570 Å for $W_6S_8(PPh_3)_6$ has been attributed to the bulkiness of the ligand that may prevent closer association with the cluster [10]. By contrast, $W_6S_8(PEt_3)_6$ has a smaller W–P distance of 2.523 Å. The phosphine binding site of dppe is more sterically hindered than that of PEt_3, but the presence of two phenyl groups instead of three makes it more accessible than that of PPh_3. Thus, it is not surprising that the W–L distance for **1**, 2.543 Å, lies midway between the values for the other two compounds. The W–W and W–L distances in **2** are within experimental uncertainties of the distances previously found in $W_6S_8(tbp)_6$ [27].
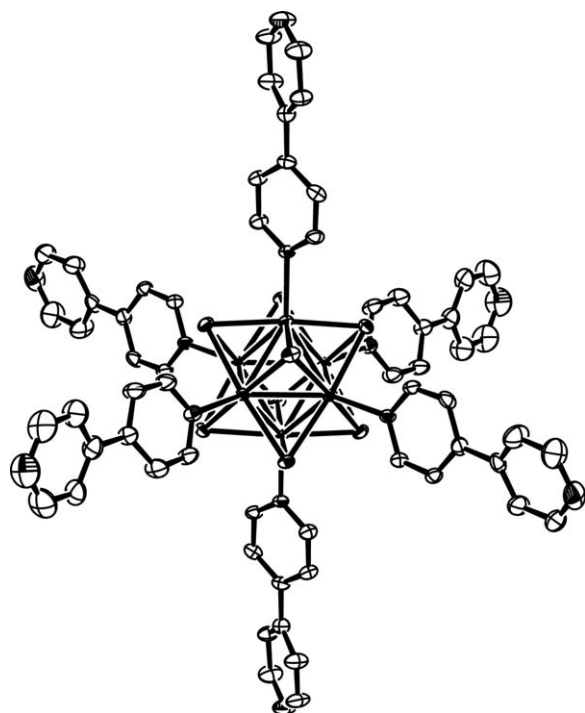
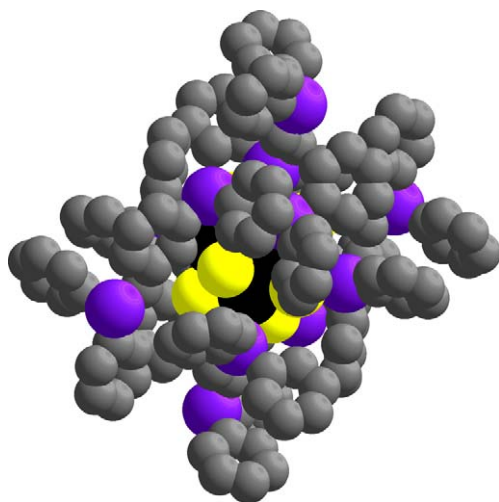Fig. 5. Molecular unit of $W_6S_8(4,4'\text{-bipy})_6$ (**2**).

Fig. 6. Space-filling model of $W_6S_8(dppe)_6$ (**1**). Color scheme: C (gray), P (purple), W (black), S (yellow).

A view of the unit cell packing for **1** as viewed along the *c*-axis is shown in Fig. 7. Clusters are centered on the cell vertices and on the (1/3, 2/3, 2/3) and (2/3, 1/3, 1/3) special positions. Because of the roughly spherical shape of the molecular unit of **1**, it is not surprising that this compound crystallizes in the $R\bar{3}$ space group.

This space group has also been found for other W_6S_8 cluster compounds, including $W_6S_8(tbp)_6$ [27] and $W_6S_8(PEt_3)_6$ [20]. A structure was also found for a single-crystal of **1** grown by layering of the reaction solution with Et_2O. The cell parameters for this structure differed slightly from the parameters reported in Table 1, with *a* = *b* = 29.8064 Å and *c* = 14.2891 Å. Arrangement of clusters within the unit cell was the same as for the structure reported here. However, this crystal was more disordered than a crystal grown by layering with acetonitrile, and the final *R*-values were higher.

The unit cell packing for **2** is shown in Fig. 8. Clusters are situated on –1 special positions. Aniline molecules of crystallization occupy the channels among clusters. A structure was also found for the **2**•2(4,4′-bipy) compound grown from a 4,4′-bipy/toluene melt. These needle-like crystals were also found to be in the *P*-1 space group, with *a* = 9.4544(11) Å, *b* = 14.6207(17) Å, *c* = 15.8388(18) Å, α = 67.703(3)°, β = 81.334(3)°, and γ = 86.142(3)°. The cell axes of this structure and that of **2**•5aniline agree within 10%, although there are bigger differences in the cell angles. Clusters are centered on the same special positions in both structures, with the main difference being the identity of the molecules of crystallization.

3.3. Powder X-ray diffraction

The insoluble $W_6S_8(dppe)_6$ powder was characterized by powder X-ray diffraction. The diffraction pattern that was collected is shown in Fig. 9, along with a pattern simulated by PowderCell [28] using the structural information found by single-crystal diffraction. Since the bulk powder was obtained from a mixture of benzene and Et_2O, the structural data used in simulating the pattern were from a single-crystal grown from this same solvent mixture. As mentioned above, these parameters are slightly different than those for a crystal grown from benzene/acetonitrile.

JADE software [29] was used to find the peak positions in the experimental pattern, allowing a quantitative comparison between the experimental and simulated data. This comparison may be seen in Table 3. There is a systematic difference between the two sets of peak positions, with the simulated 2θ values an average of 0.082° larger than the experimental values. In addition to a possible contribution from zero-point error
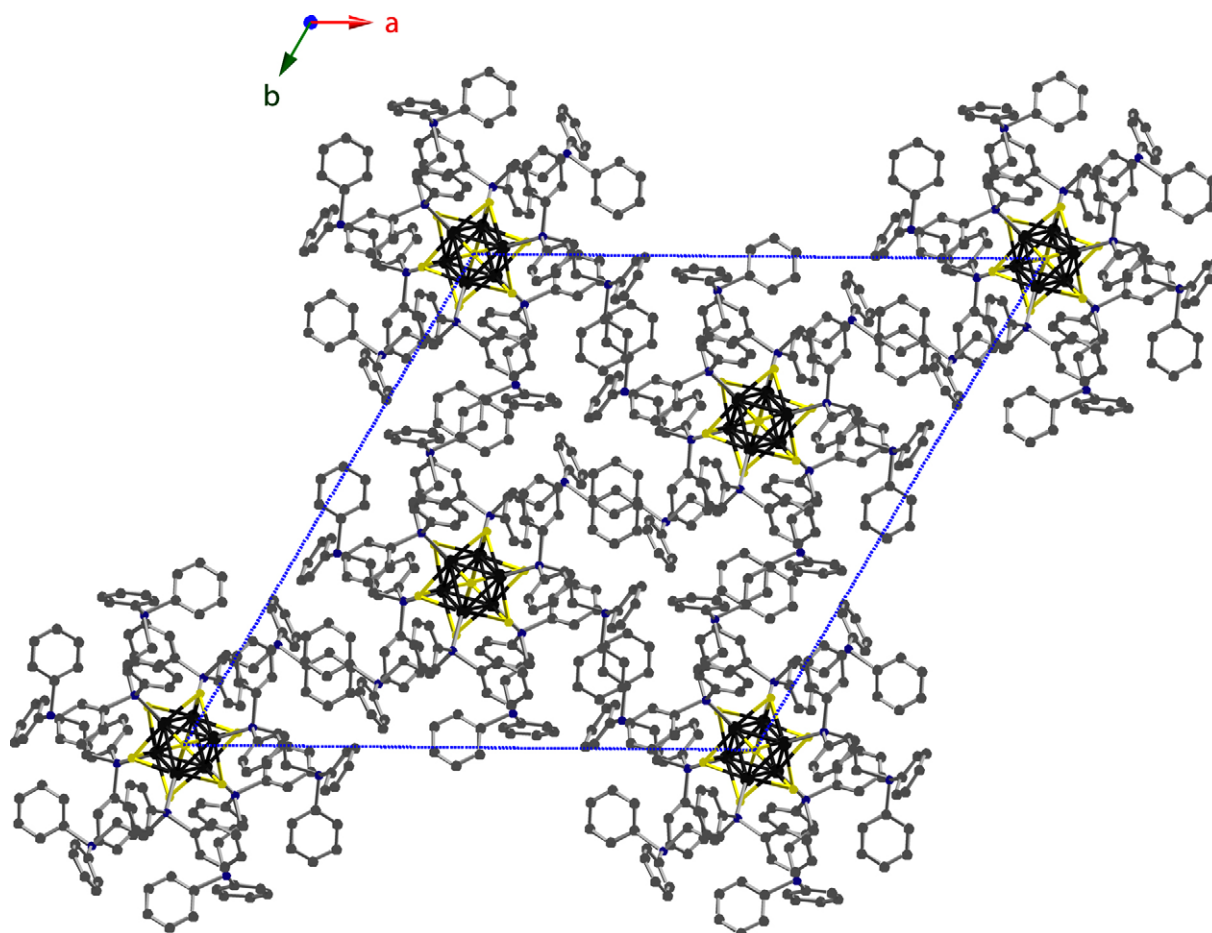
Fig. 7. Unit cell packing of $W_6S_8(dppe)_6$ (**1**), viewed along the *c*-direction.

in the X-ray diffraction measurement, this difference may arise from the fact that the powder pattern was collected at room temperature, whereas the single-crystal data were collected at 173 K. The sign of the difference that is observed is consistent with what would be expected for a small expansion of a unit cell upon warming from 173 K to room temperature.

The program Latcon-X [30] was used to determine unit cell parameters using the experimentally observed values of 2θ and the *hkl* indices obtained from the simulated pattern. This refinement found $a = b = 29.9110$ Å and $c = 14.4608$ Å. As compared with the values for a single-crystal grown from benzene/diethyl ether, these parameters show increases of 0.104 and 0.172 Å for *a* and *c*, respectively. Returning to Table 3, it may be observed that the largest differences in peak positions correspond to reflections for which *l* is large. This is consistent with the finding that $\Delta c/c$ differs more than

$\Delta a/a$ in a comparison of cell parameters from powder and single-crystal data.

Qualitatively, intensities are in fairly good agreement between the two patterns. Some differences may result from preferred orientation of crystallites in the powder sample. The good agreement between simulated and experimental patterns helps to confirm the identity of the bulk powder in the absence of NMR data.

4. Conclusions

Two new compounds, $W_6S_8(dppe)_6$ (**1**) and $W_6S_8(4,4'-bipy)_6$ (**2**) were synthesized through ligand substitution on the W_6S_8 cluster core. Both of these ligands are ditopic and could potentially coordinate to two different clusters, but the structures found here
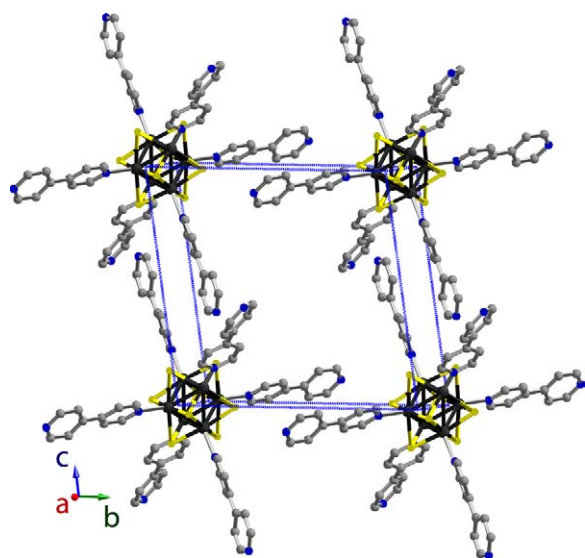
Fig. 8. Unit cell packing of $W_6S_8(4,4'\text{-bipy})_6$ (**2**), viewed approximately along the *a*-direction.

Table 3
Calculated and observed powder X-ray diffraction peak positions (degrees 2θ) for $W_6S_8(dppe)_6$ (**1**)

h k l	Experimental	Simulated	Difference (sim – exp)
1 1 0	5.905	5.926	0.021
1 0 1	6.986	7.065	0.079
2 0 –1	9.143	9.226	0.083
3 0 0	10.249	10.272	0.023
1 2 –1, 2 1 1	10.905	10.972	0.067
2 2 0	11.833	11.867	0.034
1 0 –2	12.712	12.846	0.134
3 1 –1, 1 3 1	13.750	13.824	0.074
4 0 1	14.980	15.052	0.072
2 1 –2, 1 2 2	15.220	15.359	0.139
4 1 0, 1 4 0	15.655	15.720	0.065
3 2 1, 2 3 –1	16.114	16.189	0.075
1 3 –2, 3 1 2	17.386	17.523	0.137
4 0 –2	18.367	18.512	0.145
Average difference =			0.082

show these ligands in monotopic binding modes. Use of 4,4′-bipy leads to this monotopically bound product when a large excess of the ligand is used but produces an amorphous, insoluble product when a small ligand: cluster stoichiometry is employed, presumably due to linking of clusters. Dppe behaves rather differently than 4,4′-bipy in that it does not appear to link clusters even when a low stoichiometry of the ligand per cluster is used. This suggests that the second phosphorus site is inaccessible to a second cluster due to the bulkiness of the phenyl groups and of surrounding ligands. Both compounds have been characterized structurally through single-crystal X-ray diffraction, and a powder X-ray diffraction pattern collected for bulk material of **1** agrees well with a pattern simulated from a single-crystal structure.
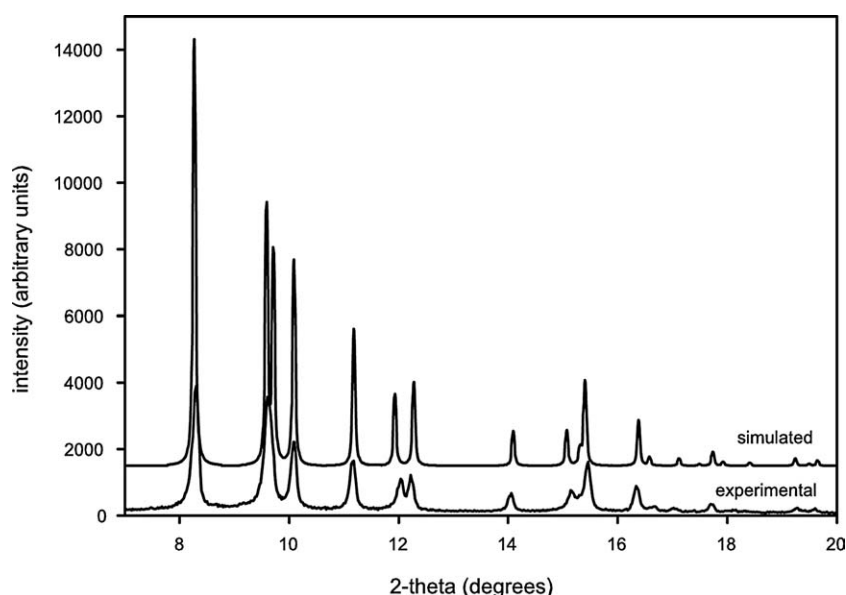

Fig. 9. Overlay of simulated and experimental powder X-ray diffraction patterns for $W_6S_8(dppe)_6$ (**1**).

References

[1] T. Saito, N. Yamamoto, T. Yamagata, H. Imoto, J. Am. Chem. Soc. 110 (1988) 1646.

[2] T. Saito, A. Yoshikawa, T. Yamagata, H. Imoto, K. Unoura, Inorg. Chem. 28 (1989) 3588.

[3] S. Hilsenbeck, V.G. Young, R.E. McCarley, Inorg. Chem. 33 (1994) 1822.

[4] Z. Xiang, R.E. McCarley, Inorg. Chem. 34 (1995) 2678.

[5] D. Venkataraman, L.L. Rayburn, L.I. Hill, S. Jin, A.-S. Malik, K.J. Turneau, F.J. DiSalvo, Inorg. Chem. 38 (1999) 828.

[6] S. Jin, F. Popp, S.W. Boettcher, M. Yuan, C.M. Oertel, F.J. DiSalvo, J. Chem. Soc., Dalton Trans. 16 (2002) 3096.

[7] T. Saito, N. Yamamoto, T. Nagase, T. Tsuboi, K. Kobayashi, T. Yamagata, H. Imoto, K. Unoura, Inorg. Chem. 29 (1990) 764.

[8] L.I. Hill, S. Jin, R. Zhou, D. Venkataraman, F.J. DiSalvo, Inorg. Chem. 40 (2001) 2660.

[9] S. Jin, D. Venkataraman, F.J. DiSalvo, Inorg. Chem. 39 (2000) 2747.

[10] S. Jin, R. Zhou, E.M. Scheuer, J. Adamchuk, L.L. Rayburn, F.J. DiSalvo, Inorg. Chem. 40 (2001) 2666.

[11] R. Chevrel, M. Sergent, J. Prigent, J. Solid-State Chem. 3 (1971) 315.

[12] R. Chevrel, M. Hirrien, M. Sergent, Polyhedron 5 (1986) 87.

[13] P.J. Mulhern, R.R. Haering, Can. J. Phys. 62 (1984) 527.

[14] D. Aurbach, Z. Lu, A. Schechter, Y. Gofer, H. Gizbar, R. Turgeman, Y. Cohen, M. Moshkovich, E. Levi, Nature 407 (2000) 724.

[15] K.F. McCarty, J.W. Anderegg, G.L. Schrader, J. Catal. 93 (1985) 375.

[16] R.K. Thompson, S.J. Hilsenbeck, T.J. Paskach, R.E. McCarley, G.L. Schrader, J. Mol. Catal. A: Chem. 161 (2000) 75.

[17] T. Hughbanks, R. Hoffmann, J. Am. Chem. Soc. 105 (1983) 1150.

[18] A.-S. Malik, Dissertation, Cornell University, USA, 1998.

[19] N. Prokopuk, D.F. Shriver, Adv. Inorg. Chem. 46 (1999) 1.

[20] L.L. Rayburn, Dissertation, Cornell University, USA, 2001.

[21] S. Jin, Dissertation, Cornell University, USA, 2002.

[22] Z. Zheng, T.G. Gray, R.H. Holm, Inorg. Chem. 38 (1999) 4888.

[23] SMART and SAINT, Data Collection and Processing Software for the SMART System, Bruker Analytical X-Ray Instruments Inc., 1995.

[24] G.M. Sheldrick, The computer program SADABS is used by Siemens CCD diffractometers, Institute für Anorganische Chemie der Universität Göttingen, Germany, 1999.

[25] G.M. Sheldrick, SHELXL-97, Institute für Anorganische Chemie der Universität Göttingen, Germany, 1999.

[26] L.J. Farrugia, J. Appl. Crystallogr. 30 (1997) 565.

[27] G.M. Ehrlich, C.J. Warren, D.A. Vennos, D.M. Ho, R.C. Haushalter, F.J. DiSalvo, Inorg. Chem. 34 (1995) 4454.

[28] W. Krause, G. Nolze, PowderCell, version 2.4, Federal Institute for Materials Research and Testing, Berlin, 2000.

[29] Jade version 6.0, Materials Data, Inc., Livermore, CA, 1995.

[30] D. Schwarzenbach, G. King, LATCON-X, Heverlee, Belgium.